IMPLICIT–EXPLICIT BDF METHODS FOR THE KURAMOTO–SIVASHINSKY EQUATION

GEORGIOS AKRIVIS AND YIORGOS-SOKRATIS SMYRLIS

Abstract. We consider the periodic initial value problem for the Kuramoto–Sivashinsky (KS) equation. We approximate the solution by discretizing in time by implicit–explicit BDF schemes and in space by a pseudo–spectral method. We present the results of various numerical experiments.

1. Introduction

Linearly implicit methods for a class of nonlinear parabolic equations were recently constructed and analyzed in [3], [4] and [2] under various conditions on the nonlinearity and the schemes. These schemes are efficient and unconditionally stable. These schemes were not implemented in [2], [3] and [4].

In this paper we focus on a concrete example, namely the periodic initial value problem for the Kuramoto–Sivashinsky (KS) equation, and its discretization in time by combinations of backward differentiation formulae (BDF) and appropriate explicit schemes. In space we discretize by a pseudo–spectral method. In this study we implement these schemes and present the results of various numerical experiments. Our experiments establish the $p-$th order of accuracy of the $p-$step BDF scheme and reproduce efficiently the universal attractors of the equation. Certain quantitative characteristics of the universal attractors are calculated with the same order of accuracy.

We consider the periodic initial value problem for the KS equation: We seek a real-valued function $u = u(x,t)$, defined on $\mathbb{R} \times \mathbb{R}_0^+$, satisfying

$$u_t + uu_x + u_{xx} + \nu u_{xxxx} = 0 \quad \text{for} \quad (x,t) \in \mathbb{R} \times \mathbb{R}_0^+ \tag{1.1}$$

$$u(\cdot, 0) = u^0 \tag{1.2}$$

with $u^0 : \mathbb{R} \to \mathbb{R}$ a sufficiently smooth, $2\pi-$periodic function and ν a positive parameter playing the role of viscosity. The solution of (1.1)–(1.2) will also be $2\pi-$periodic in space, i.e. $u(x + 2\pi, t) = u(x,t)$ for all $x \in \mathbb{R}$ and $t \geq 0$.

KS is a simple partial differential equation (PDE) exhibiting a particularly complex dynamical behaviour as the viscosity parameter ν varies. It arises as an amplitude equation

Date: June 16, 2013.

Key words and phrases. Kuramoto–Sivashinsky equation, Implicit-explicit BDF methods, Periodic attractors, Period doubling cascades.

in long-wave, weakly nonlinear stability analysis, in a great variety of applications. For example it arises in concentration waves in chemically reacting systems [17], in flame propagation and reaction combustion [24], in free surface film-flows of viscous liquids, and in the dynamics of interfaces in two-phase flows in cylindrical geometries [22]. It is one of the simplest PDEs with a convective nonlinearity and a band of unstable modes, in its linearized version (around zero), and thus it has served as an appropriate example on which the general notions of inertial manifold theory are applied. This means that the long time dynamic behaviour of KS is captured well by a finite dimensional dynamical system, the number of degrees of freedom of which is at least as large as the number of linearly unstable Fourier frequencies [8]. For $2\pi-$periodic solutions the number of linearly unstable frequencies is $[\nu^{-1/2}]$ while the best estimate for the dimension of the inertial manifold is $O(\nu^{-21/40})$ in the case of solutions of odd parity, i.e., $u(-x,t) = -u(x,t)$, [8]. This bound is useful in determining estimates of the Hausdorff dimension of the universal attractor.

The boundedness of the solutions of the KS equation, for general initial data, has been proved independently by Il'yashenko [13], Goodman [9] and Collet et al [6]. The best estimate for the Hausdorff dimension of the attractor so far appears in [6]. In this work it is proved that

$$\limsup_{t\to+\infty} \|u(\cdot,t)\| \;\le\; c\cdot\nu^{-13/10},$$

with $\|\cdot\|$ denoting the L^2-norm of $2\pi-$periodic functions and c a positive constant, independent of u_0 and ν. Similar boundedness results can be derived for any Sobolev norm of the solution. The analyticity of the solution has also been proved by Collet et al [7]. In the case of the rescaled $L-$periodic KS equation

$$U_t + UU_x + U_{xx} + U_{xxxx} = 0\,, \tag{1.3}$$

it is proved that, for sufficiently large t, the function $U(\cdot,t)$ is analytic in a strip of width $\beta \ge cL^{-16/25}$ around the real axis, which in turn implies that the high frequency part of the spectrum has the form

$$|\hat{U}(j,t)| \;=\; O\left(\mathrm{e}^{-c\,L^{-16/25}q|j|}\right),$$

where $\hat{U}(j,t)$ is the $j-$th Fourier coefficient of $U(\cdot,t)$ and $q = 2\pi/L$. A series of numerical experiments in [7] indicate the presence of a much stronger bound, namely, that there exists a $\beta > 0$, independent of L, such that the solutions of (1.3) satisfy

$$\limsup_{t\to+\infty} \sum_{j\in\mathbb{Z}} \mathrm{e}^{2\beta q|j|}\,|\hat{U}(j,t)|^2 \;<\; \infty \tag{1.4}$$

and numerical computations indicate that $\beta \approx 3.5$. Straightforward calculations show that if $U(x,t)$ is a solution of (1.3), then

$$u(x,t) \;=\; \frac{L}{2\pi}U\left(\frac{L}{2\pi}x, \frac{L^2}{4\pi^2}t\right)$$

is a $2\pi-$periodic solution of the KS equation for $\nu = \left(\frac{2\pi}{L}\right)^2$. Similarly, if $\hat{u}(j,t)$ is the $j-$th Fourier coefficient of u then $\hat{u}(j,t) = \hat{U}(j, \frac{L^2}{4\pi^2}t)$. Therefore (1.4) implies that

$$\limsup_{t\to+\infty} |\hat{u}(j,t)| \le M\mathrm{e}^{-\beta\sqrt{\nu}|j|}, \tag{1.5}$$

for some positive constant M. This bound has been extremely useful in the present work in the numerical experiments. The truncation of the high Fourier coefficients becomes plausible and the number of the frequencies kept could be determined by (1.5). Nevertheless, in our work, we have carried out extensive numerical experiments in order to determine how many modes contribute numerically to the solution, as shown in Figure 1.

The KS equation has been studied numerically by many authors, see [11], [12], [14], [16], [23], [25], [26]. While the space discretization has been consistently carried out via spectral methods, many different methods have been used for the time discretization including Runge–Kutta methods of different orders (for example the subroutine `radau5` which is based on the Runge–Kutta–Radau IIA method of order 5 with step size control[1] [10]) and a split scheme of variable time step, according to the Strang–split method, integrating the linear and nonlinear parts separately, exploiting the fact that the linear part can be integrated exactly in the Fourier space [25], [26]. The numerical studies have revealed extremely interesting low-dimensional dynamic behaviour, including stationary and travelling waves, complicated time-periodic attractors, a variety of quasi-periodic attractors, homoclinic bursts and various chaotic attractors. Several transitions to chaos have been reported, including the one via period doubling cascades [25], [26].

Explicit multistep or Runge–Kutta schemes are unstable for (1.1) and may be only conditionally stable in the fully discrete case, i.e., when we discretize in space as well, under very restrictive conditions on the size of kh^{-4}, with k denoting the time step and h the space discretization parameter. Implicit schemes on the other hand may be unconditionally stable but their implementation requires solving nonlinear problems at every time step; these problems reduce to nonlinear systems in the fully discrete case. In this paper we discretize in time by a combination of implicit and explicit schemes leading to unconditionally stable, linearly implicit schemes.

With $Av = \nu v_{xxxx} + v_{xx} + \frac{1}{\nu}v$ and $B(v) = -vv_x + \frac{1}{\nu}v$, the KS equation may be written in the form

$$u_t + Au = B(u). \tag{1.6}$$

We discretize the linear part $v_t + Av = 0$ of (1.6) by $p-$step BDF schemes, $p \le 6$, and the nonlinear part $v_t = B(v)$ by appropriate explicit schemes; this leads to unconditionally stable schemes of order p.

The paper is organized as follows. In Section 2 we describe the numerical schemes used. Time discretization is obtained via stable $p-$step implicit–explicit BDF methods,

[1]This subroutine, together with its implementations, which include the KS equation, can be found in the web page of E. Hairer: `http://www.unige.ch/math/folks/hairer/testset/testset.html`

$p = 1, \ldots, 6$, whereas in space we use pseudo–spectral methods. In Section 3 we present numerical experiments which establish the $p-$th order of accuracy of the $p-$step BDF method via a suitably modified *inhomogeneous* problem where the solution is known. We have carried out specific experiments in order to assess the number of modes to be used, for different values of ν. We have also reproduced results of previously reported numerical experiments, through extensive computations. We do obtain the same universal attractors, at a significantly smaller cost. Finally in Section 4, we give some concluding remarks and suggest certain other possibilities.

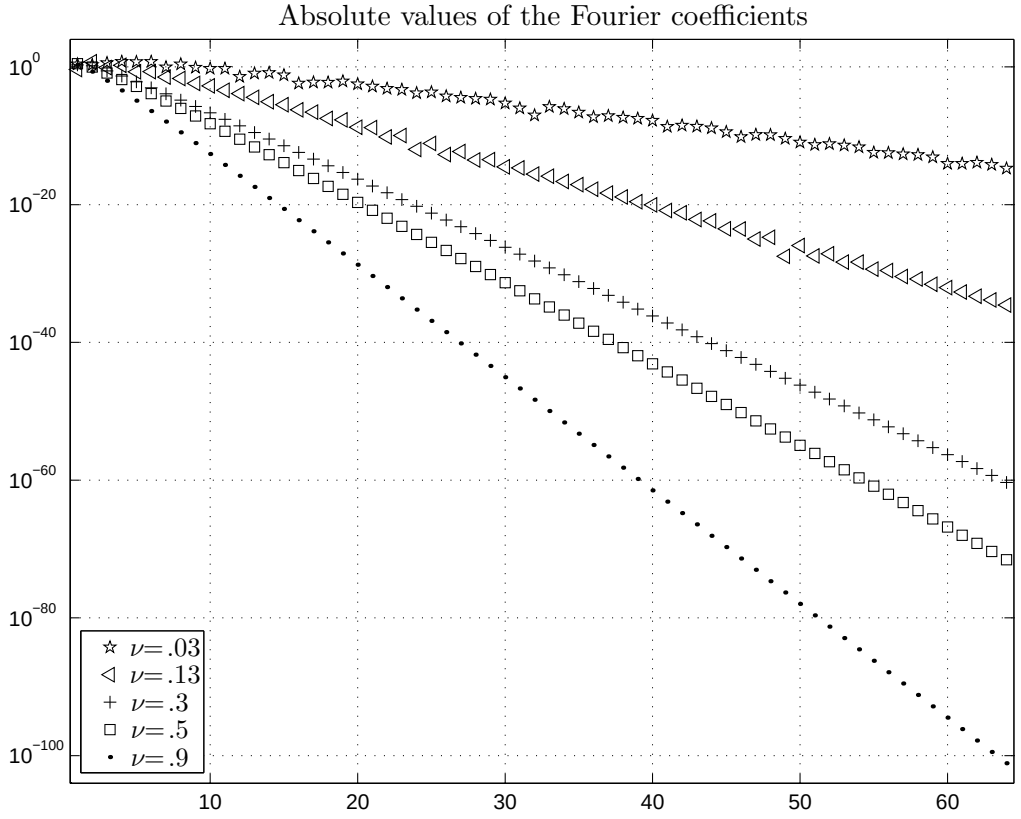

FIGURE 1. The spectrum of the solution of KS for different values of the parameter ν. The `log-plot` shows that the Fourier modes decay exponentially fast; slower as ν decreases.

2. The numerical schemes

In this section we present the numerical schemes, first the time stepping schemes and subsequently the fully discrete schemes.

2.1. **Discretization in time.** For $p \in \{1,2,3,4,5,6\}$, the polynomials α, β and γ are given by

$$\alpha(\zeta) := \sum_{j=1}^{p} \frac{1}{j}\zeta^{p-j}(\zeta-1)^j, \quad \beta(\zeta) := \zeta^p \quad \text{and} \quad \gamma(\zeta) := \zeta^p - (\zeta-1)^p.$$

Let α_j and γ_j denote the coefficients of ζ^j of the polynomials α and γ, respectively. The $(\alpha,\beta)-$scheme described by the polynomials α and β is the $p-$step BDF scheme; these schemes are strongly $A(0)-$stable and will be used for the discretization of the linear part of (1.5). The explicit scheme (α,γ) will be used for the discretization of the nonlinear part of (1.5). Let us note that this particular choice of the polynomial γ is motivated by the fact that, for the given $(\alpha,\beta)-$scheme, it is the only choice leading to a $p-$step implicit–explicit (α,β,γ) scheme of order p, see [3].

Let $T > 0$, k denote the time step, $N \in \mathbb{N}$ be such that $Nk = T$, and $t^n := nk, n = 0,\dots,N$. We use the (α,β,γ) scheme to define approximations U^n to $u(t^n)$ by

$$\sum_{i=0}^{p} \alpha_i U^{n+i} + kAU^{n+p} = k\sum_{i=0}^{p-1} \gamma_i B(U^{n+i}),\ n = 0,\dots,N-p, \tag{2.1}$$

for given initial approximations $U^0,\dots,U^{p-1}$. Since $\alpha_p > 0$ and the operator A is positive definite, the approximations $U^p,\dots,U^N$ are well defined by (2.1).

For $p = 1,\dots,6$, the scheme (2.1) takes the following form, respectively,

$$U^{n+1} + kAU^{n+1} = U^n + kB(U^n), \tag{2.2}$$

$$\frac{3}{2}U^{n+2} + kAU^{n+2} = 2U^{n+1} - \frac{1}{2}U^n + 2kB(U^{n+1}) - kB(U^n), \tag{2.3}$$

$$\begin{aligned}\frac{11}{6}U^{n+3} + kAU^{n+3} = {} & 3U^{n+2} - \frac{3}{2}U^{n+1} + \frac{1}{3}U^n \\ & + 3kB(U^{n+2}) - 3kB(U^{n+1}) + kB(U^n),\end{aligned} \tag{2.4}$$

$$\begin{aligned}\frac{25}{12}U^{n+4} + kAU^{n+4} = {} & 4U^{n+3} - 3U^{n+2} + \frac{4}{3}U^{n+1} - \frac{1}{4}U^n \\ & + 4kB(U^{n+3}) - 6kB(U^{n+2}) + 4kB(U^{n+1}) - kB(U^n),\end{aligned} \tag{2.5}$$

$$\begin{aligned}&\frac{137}{60}U^{n+5} + kAU^{n+5} = 5U^{n+4} - 5U^{n+3} + \frac{10}{3}U^{n+2} - \frac{5}{4}U^{n+1} + \frac{1}{5}U^n \\ &+ 5kB(U^{n+4}) - 10kB(U^{n+3}) + 10kB(U^{n+2}) - 5kB(U^{n+1}) + kB(U^n),\end{aligned} \tag{2.6}$$

$$
\begin{aligned}
\frac{147}{60}U^{n+6} + kAU^{n+6} &= 6U^{n+5} - \frac{15}{2}U^{n+4} + \frac{20}{3}U^{n+3} - \frac{15}{4}U^{n+2} \\
&+ \frac{6}{5}U^{n+1} - \frac{1}{6}U^n + 6kB(U^{n+5}) - 15kB(U^{n+4}) \\
&+ 20kB(U^{n+3}) - 15kB(U^{n+2}) + 6kB(U^{n+1}) - kB(U^n).
\end{aligned} \tag{2.7}
$$

Scheme (2.2) is obviously a combination of the implicit and the forward Euler methods.

For $s \in \mathbb{N}_0$, let $H^s_{\rm per}$ denote the periodic Sobolev space of order s, consisting of the $2\pi-$periodic elements of $H^s_{\rm loc}(\mathbb{R})$, and let $\|\cdot\|_{H^s}$ be the norm over a period in $H^s_{\rm per}$. The inner product in $H := L^2_{\rm per} = H^0_{\rm per}$ is denoted by $(\cdot,\cdot)$, and the induced norm by $\|\cdot\|$. As already mentioned, we let $A : H^4_{\rm per} \to H$ be defined by $Av := \nu v_{xxxx} + v_{xx} + \frac{1}{\nu}v$. Then $V := D(A^{1/2}) = H^2_{\rm per}$, and the norm $|\!|\!|\cdot|\!|\!|, |\!|\!|v|\!|\!| := \|A^{1/2}v\|$, in V is given by

$$
|\!|\!|v|\!|\!| \;=\; \left(\nu\|v_{xx}\|^2 - \|v_x\|^2 + \frac{1}{\nu}\|v\|^2\right)^{1/2}.
$$

It is easily seen that

$$
\|v_x\|^2 \le \frac{\nu}{2}\|v_{xx}\|^2 + \frac{1}{2\nu}\|v\|^2 \qquad \text{for all } v \in V;
$$

therefore

$$
(Av, v) \;\ge\; \frac{1}{2}\left(\nu\|v_{xx}\|^2 + \frac{1}{\nu}\|v\|^2\right) \qquad \text{for all } v \in V, \tag{2.8}
$$

and thus, A is positive definite.

Further, let $B : V \to H$ be given by $B(v) := -vv_x + \frac{1}{\nu}v$. Then,

$$
B(v) - B(w) \;=\; -\frac{1}{2}(v^2 - w^2)_x + \frac{1}{\nu}(v - w)\,,
$$

and thus by periodicity, for $\omega \in V$,

$$
(B(v) - B(w), \omega) = \frac{1}{2}(v^2 - w^2, \omega_x) + \frac{1}{\nu}(v - w, \omega)\,,
$$

and therefore,

$$
(B(v) - B(w), \omega) \le \frac{1}{2}\|v + w\|\,\|v - w\|\,\|\omega_x\|_{L^\infty} + \frac{1}{\nu}\|v - w\|\,\|\omega\|\,. \tag{2.9}
$$

Now, since ω_x vanishes at some point in the interval $(0, 2\pi)$, it is easily seen that

$$
\|\omega_x\|_{L^\infty} \le \sqrt{2\pi}\,\|\omega_{xx}\|,
$$

and (2.9) yields

$$
(B(v) - B(w), \omega) \le \frac{\sqrt{2\pi}}{2}\|v + w\|\,\|v - w\|\,\|\omega_{xx}\| + \frac{1}{\nu}\|v - w\|\,\|\omega\|\,. \tag{2.10}
$$

We identify H with its dual, and denote by V' the dual of V, again by $(\cdot,\cdot)$ the duality pairing between V' and V, and by $|\!|\!| \cdot |\!|\!|_\star$ the dual norm on V'. Since, obviously,

$$\sqrt{\frac{\nu}{2}}\,\|\omega_{xx}\| \le |\!|\!|\omega|\!|\!|, \qquad \frac{1}{\sqrt{2\nu}}\,\|\omega\| \le |\!|\!|\omega|\!|\!|, \qquad \text{for all } \ \omega \in V,$$

we conclude from (2.10) that

$$|\!|\!| B(v) - B(w) |\!|\!|_\star \le \frac{1}{\sqrt{\nu}}\Big[\sqrt{\pi}\|v+w\| + \sqrt{2}\Big]\,\|v-w\|\,. \tag{2.11}$$

Let T_u be a tube around the solution u defined in terms of the norm of H, i.e.

$$T_u \,:=\, \Big\{\, v \in V \,:\, \min_t \|u(t) - v\| \le 1 \,\Big\}\,.$$

Obviously, for $v, w \in T_u$, we have

$$\|v+w\| \;\le\; 2 + 2\max_{0\le t\le T}\|u(t)\|\,,$$

and (2.11) yields

$$|\!|\!| B(v) - B(w) |\!|\!|_\star \;\le\; \mu\|v-w\| \tag{2.12}$$

with

$$\mu := \frac{1}{\sqrt{\nu}}\,\left[2\sqrt{\pi}\,\left(1 + \max_{0\le t\le T}\|u(t)\|\right) + \sqrt{2}\right]\,. \tag{2.13}$$

Assume now that we are given starting approximations $U^0, \ldots, U^{p-1}$ satisfying

$$\sum_{j=0}^{p-1}\|u(t^j) - U^j\| \;\le\; Ck^p\,. \tag{2.14}$$

Then, the theory of [2], see also [4] and [3], yields the optimal order error estimate

$$\max_{0\le n\le N}\|u(t^n) - U^n\| \;\le\; ck^p. \tag{2.15}$$

We emphasize that (2.14) suffices here since on the right-hand side of (2.12) only the norm $\|\cdot\|$ appears, i.e., in the notation of [2] we have $\lambda = 0$, and also $\beta(\zeta) = \zeta^p$, i.e., all coefficients of β but the one of ζ^p vanish, see Remark 7.2 in [2].

Remark 2.1. In the experiments we will also discretize the equation

$$u_t + uu_x + u_{xx} + \nu u_{xxxx} = f(x,t) \quad \text{in} \quad \mathbb{R}\times\mathbb{R}_0^+\,.$$

In this case the schemes (2.2)–(2.7) are modified by adding the term $kf(t^{n+p})$ to their right-hand sides, p being the order of the scheme. Alternatively, f could have been incorporated into B.

Starting approximations. For the error estimate (2.15) to hold, we need starting approximations $U^1,\dots,U^{p-1}$, for $p=2,\dots,6$, satisfying (2.14). We present here some choices leading to such approximations.

The first choice is based on a Taylor expansion and requires, for $p>2$, the calculation of higher-order derivatives of the initial value u^0. Assume that u^0 is sufficiently smooth such that one can calculate the time derivatives $u^{(j)}(0)$, $j=1,\dots,p-1$, of the exact solution at $t=0$. Then, it is easily seen that $U^0=u^0$ and $U^j=T_j^p u(0)$, with

$$T_j^p u(0) := u^0 + jku^{(1)}(0) + \cdots + \frac{(jk)^{p-1}}{(p-1)!}u^{(p-1)}(0), \quad j=1,\dots,p-1,$$

satisfy (2.14). This choice might be inconvenient in applications since it requires high order time derivatives of the solution u.

Another way leading to appropriate starting approximations is the use of linearly implicit Runge–Kutta schemes of order at least $p-1$ for the computation of $U^1,\dots,U^{p-2}$, cf. [18], [15]; U^{p-1} can be computed by the $(p-1)-$step implicit–explicit scheme. Let us note that, due to the periodic boundary conditions, the Runge–Kutta schemes do not suffer from order reduction in this case, cf. [1]. Also note that schemes of order $p-1$, when applied a fixed number of steps yield approximations of order p.

As already mentioned, for the second order scheme (2.3), we may compute U^1 by performing one step by the first order scheme (2.2), i.e., we let U^1 be given by

$$U^1 + kAU^1 = u^0 + kB(u^0). \tag{2.3–1}$$

Let us also briefly discuss two convenient ways leading to appropriate starting approximations for the third order scheme. In this case, we need third order starting approximations U^1 and U^2. Once U^1 has been calculated, we may perform one step with the second-order scheme (2.3) to get U^2. For U^1, we start with the second order approximations $u^0+ku_t(0)$ to $u(k)$ and $u^0u_x^0+k\big(u^0u_t(0)\big)_x$ to $u(k)u_x(k)$, and perform one step with a linearly implicit modified second order Crank–Nicolson scheme to obtain U^1 by

$$U^1 + \frac{1}{2}kAU^1 = u^0 - \frac{1}{2}kAu^0 + kB(u^0) + \frac{1}{2\nu}k^2u_t(0) - \frac{1}{2}k^2\big(u^0u_t(0)\big)_x. \tag{2.4–1}$$

The next starting approximation U^2 may then be calculated by

$$\frac{3}{2}U^2 + kAU^2 \;=\; 2U^1 - \frac{1}{2}u^0 + 2kB(U^1) - kB(u^0). \tag{2.4–2}$$

In (2.4–1) the time derivative of u is used. An alternative way of defining a third order approximation U^1 to $u(k)$, avoiding the use of time derivatives, is as follows: We begin with a second order approximation $\tilde U^1$, computed by the implicit–explicit Euler scheme (2.2),

$$\tilde U^1 + kA\tilde U^1 = u^0 + kB(u^0), \tag{2.4–1$'$}$$

and correct it to a third order approximation by the linearly implicit Crank–Nicolson scheme,

$$\frac{1}{k}(U^1 - u^0) + \frac{1}{2}A(U^1 + u^0) = B(\frac{1}{2}(\tilde{U}^1 + u^0)),$$

i.e., by

$$U^1 + \frac{1}{2}kAU^1 \;=\; u^0 - \frac{1}{2}kAu^0 + kB(\frac{1}{2}(\tilde{U}^1 + u^0)). \tag{2.4–1″}$$

2.2. **Discretization in space.** The spatially $2\pi-$periodic initial data assumption of the initial value problem enables us to represent the solution u of the KS equation in the form

$$u(x,t) \;=\; \sum_{j=1}^{\infty} ((\alpha_j(t)\cos jx + \beta_j(t)\sin jx) + \alpha_0(t)\,.$$

The term $\alpha_0(t)$ remains constant due to the conservative nature of KS. On the other hand, whenever $u(x,t)$ is a solution then so is $u(x-ct,t)+c$, which allows us to assume $\alpha_0(t) = 0$, for simplicity. Replacing $u(\cdot,t)$ by its Fourier series in the PDE we obtain

$$\begin{aligned} &u_t+uu_x + u_{xx} + \nu u_{xxxx} \;= \\ &\quad \sum_{j=1}^{\infty} \left[\alpha_j' - (j^2 - \nu j^4)\alpha_j - A_j)\cos jx + (\beta_j' - (j^2 - \nu j^4)\beta_j - B_j)\sin jx\right] \end{aligned}$$

with

$$\begin{aligned} A_j &= -\frac{j}{2}\sum_{m+n=j}\alpha_m\beta_n + \frac{j}{2}\sum_{m-n=j}(\alpha_m\beta_n - \alpha_n\beta_m) \\ B_j &= \frac{j}{4}\sum_{m+n=j}(\alpha_m\alpha_n - \beta_m\beta_n) + \frac{j}{2}\sum_{m-n=j}(\alpha_m\alpha_n + \beta_m\beta_n)\,, \end{aligned}$$

for $j \in \mathbb{N}$. Thus KS equation is transformed into an infinite dimensional system of ordinary differential equations (ODEs):

$$\begin{cases} \alpha_j' = \lambda_j\alpha_j + A_j \\ \beta_j' = \lambda_j\beta_j + B_j \end{cases} \qquad \text{for } j \in \mathbb{N}$$

and

$$A_j \;=\; A_j(\alpha_1,\alpha_2,...,\beta_1,\beta_2,...) \quad \text{and} \quad B_j \;=\; B_j(\alpha_1,\alpha_2,...,\beta_1,\beta_2,...)$$

and $\lambda_j = j^2 - \nu j^4$ are the *eigenvalues* of the linear operator. The algebraic growth of the eigenvalues makes the system stiff. All the spatial Sobolev norms of the solution of the KS equation remain bounded for all times, see [13], [9], [6]. Thus

$$\omega_j \;=\; \limsup_{t\to+\infty} |\alpha_j^2 + \beta_j^2|^{\frac{1}{2}}\,, \quad j \in \mathbb{N}\,,$$

remain bounded for all times. In particular, the Collet et al [7] proof of the analyticity of the solutions of the KS equation, implies that the ω_j's decay exponentially with respect to j. They have also presented numerical evidence in [7] that the number of determining

Fourier coefficients is proportional to $\nu^{-1/2}$. This work enables one to approximate the solution of the KS equation by truncation of the higher Fourier frequencies.

By applying the Fourier transform to $u(x,t)$ we have

$$\frac{d}{dt}\hat{u}(j) = \lambda_j \hat{u}(j) - \widehat{(uu_x)}(j)\,.$$

Thus for $j > \nu^{-1/2}$ we easily obtain

$$\limsup_{t\to+\infty} |\hat{u}(j)| \;\le\; \frac{1}{\lambda_j} \limsup_{t\to+\infty} |\widehat{(uu_x)}(j)| \;=\; \frac{j}{2\lambda_j} \limsup_{t\to+\infty} \left| \widehat{\left(u^2\right)}(j) \right| .$$

The above inequality provides a first (crude) estimate of the number of *significant* Fourier coefficients. Nevertheless, according to our numerical experiments with various schemes, a small multiple of $[\nu^{-1/2}]$ suffices for calculations in double precision. In our numerical experiments, we use at least $4\nu^{-1/2}$ Fourier modes. In fact the number of modes in our experiments is an integer of the form 2^m or $3{\cdot}2^m$, so that the FFT is efficiently implemented for the nonlinear term.

The computed value of the nonlinear terms A_j and B_j via the pseudo–spectral method is

$$A_j^N = -\frac{j}{2}\sum_{m=1}^{j-1} \alpha_m \beta_{j-m} + \frac{j}{2}\sum_{m=1}^{N-j} (\alpha_{m+j}\beta_m - \alpha_m \beta_{m+j})\,,$$

$$B_j^N = \frac{j}{4}\sum_{m=1}^{j-1} (\alpha_m \alpha_{j-m} - \beta_m \beta_{j-m}) + \frac{j}{2}\sum_{m=1}^{N-j} (\alpha_m \alpha_{m+j} + \beta_m \beta_{m+j})\,.$$

Note that in the nonlinear part of the system of ODEs corresponding to high frequencies in the truncated system, i.e., A_j^N, B_j^N, most of the contribution comes from the low frequencies, even for j large. This implies that higher frequencies are *slaved* by the low frequencies, which is one of the most typical characteristics of dissipative infinite dimensional dynamical systems. Nevertheless, we wish to allow to the high frequencies, as much freedom as possible in order to develop individual behaviour.

2.3. **Fully discrete schemes.** Let $\mu_j := \nu j^4 - j^2 + \frac{1}{\nu}$. We now present the fully discrete schemes, for $p = 1, \dots, 6$. For $p \le 3$, we also give the starting approximations, except for the first one which is the initial value.

The first order scheme is

$$\left(1 + k\mu_j\right)\hat{u}_j^{n+1} \;=\; \left(1 + \frac{1}{\nu}k\right)\hat{u}_j^n - k\widehat{(u^n u_x^n)}_j\,. \tag{2.16}$$

The second order scheme takes the form

$$\left(1 + k\mu_j\right)\hat{u}_j^1 \;=\; \left(1 + \frac{1}{\nu}k\right)\hat{u}_j^0 - k\widehat{(u^0 u_x^0)}_j\,, \tag{2.17–1}$$

cf. (2.3–1), and

$$\left(\frac{3}{2}+k\mu_j\right)\hat{u}_j^{n+2} \;=\; 2\left(1+\frac{1}{\nu}k\right)\hat{u}_j^{n+1}-\left(\frac{1}{2}+\frac{1}{\nu}k\right)\hat{u}_j^{n}-2k\widehat{(u^{n+1}u_x^{n+1})}_j+k\widehat{(u^nu_x^n)}_j\,. \tag{2.17}$$

The approximation u^1 for the third order scheme can be calculated from

$$\begin{aligned}\left(1+\frac{1}{2}k\mu_j\right)\hat{u}_j^1 = \left(1+\left(\frac{1}{\nu}-\frac{1}{2}\mu_j\right)k\right)\hat{u}_j^0 - k\widehat{(u^0u_x^0)}_j \\ +\frac{1}{2\nu}k^2\widehat{\big(u_t(0)\big)}_j+\mathrm{i}\frac{1}{2}k^2\widehat{\big(u^0u_t(0)\big)}_j\,,\end{aligned} \tag{2.18–1}$$

cf. (2.4–1), or, alternatively, from

$$(1+k\mu_j)\widehat{(\tilde{u}^1)}_j \;=\; \left(1+\frac{1}{\nu}k\right)\hat{u}_j^0-k\widehat{(u^0u_x^0)}_j \tag{2.18–1$'$}$$

and

$$\left(1+\frac{1}{2}k\mu_j\right)\hat{u}_j^1=\left(1+\frac{1}{2}\left(\frac{1}{\nu}-\mu_j\right)k\right)\hat{u}_j^0+\frac{1}{2\nu}\widehat{(\tilde{u}^1)}_j-\frac{1}{4}k\widehat{\big((\tilde{u}^1+u^0)(\tilde{u}_x^1+u_x^0)\big)}_j\,, \tag{2.18–1$''$}$$

cf. (2.4–1$'$) and (2.4–1$''$), the approximation u^2 by

$$\left(\frac{3}{2}+k\mu_j\right)\hat{u}_j^2 \;=\; 2(1+\frac{1}{\nu}k)\hat{u}_j^1-\left(\frac{1}{2}+\frac{1}{\nu}k\right)\hat{u}_j^0-2k\widehat{(u^1u_x^1)}_j+k\widehat{(u^0u_x^0)}_j\,, \tag{2.18–2}$$

cf. (2.4–2), and the other approximations by

$$\begin{aligned}\left(\frac{11}{6}+k\mu_j\right)\hat{u}_j^{n+3} = 3\left(1+\frac{1}{\nu}k\right)\hat{u}_j^{n+2}-3\left(\frac{1}{2}+\frac{1}{\nu}k\right)\hat{u}_j^{n+1}+\left(\frac{1}{3}+\frac{1}{\nu}k\right)\hat{u}_j^n \\ -3k\widehat{(u^{n+2}u_x^{n+2})}_j+3k\widehat{(u^{n+1}u_x^{n+1})}_j-k\widehat{(u^nu_x^n)}_j\,.\end{aligned} \tag{2.18}$$

For the fourth, fifth and sixth order schemes we do not give specific choices of starting approximations, but we only give the general step of the schemes. The fourth order scheme is

$$\begin{aligned}&\left(\frac{25}{12}+k\mu_j\right)\hat{u}_j^{n+4} \;=\; 4\left(1+\frac{1}{\nu}k\right)\hat{u}_j^{n+3}-6\left(\frac{1}{2}+\frac{1}{\nu}k\right)\hat{u}_j^{n+2}\\ &+4\left(\frac{1}{3}+\frac{1}{\nu}k\right)\hat{u}_j^{n+1}-\left(\frac{1}{4}+\frac{1}{\nu}k\right)\hat{u}_j^{n}-4k\widehat{(u^{n+3}u_x^{n+3})}_j\\ &+6k\widehat{(u^{n+2}u_x^{n+2})}_j-4k\widehat{(u^{n+1}u_x^{n+1})}_j+k\widehat{(u^nu_x^n)}_j,\end{aligned} \tag{2.19}$$

the fifth order scheme is

$$\begin{aligned}&\left(\frac{137}{60}+k\mu_j\right)\hat{u}_j^{n+5} \;=\; 5\left(1+\frac{1}{\nu}k\right)\hat{u}_j^{n+4}-10\left(\frac{1}{2}+\frac{1}{\nu}k\right)\hat{u}_j^{n+3}\\ &+10\left(\frac{1}{3}+\frac{1}{\nu}k\right)\hat{u}_j^{n+2}-5\left(\frac{1}{4}+\frac{1}{\nu}k\right)\hat{u}_j^{n+1}+\left(\frac{1}{5}+\frac{1}{\nu}k\right)\hat{u}_j^{n}-5k\widehat{(u^{n+4}u_x^{n+4})}_j\\ &+10k\widehat{(u^{n+3}u_x^{n+3})}_j-10k\widehat{(u^{n+2}u_x^{n+2})}_j+5k\widehat{(u^{n+1}u_x^{n+1})}_j-k\widehat{(u^nu_x^n)}_j,\end{aligned} \tag{2.20}$$

Order	$k=\frac{1}{10}$	$k=\frac{1}{20}$	$k=\frac{1}{40}$	$k=\frac{1}{80}$	$k=\frac{1}{160}$	$k=\frac{1}{320}$
1	.3639	.1979	.1034	.5291e-1	.2676e-1	.1346e-1
2	.3903e-1	.1017e-1	.2584e-2	.6505e-3	.1631e-3	.4085e-4
3	.4013e-2	.5102e-3	.6430e-4	.8070e-5	.1011e-5	.1265e-6
4	.4567e-3	.2862e-4	.1790e-5	.1119e-6	..6997e-8	.4374e-9
5	.6826e-4	.2123e-5	.6610e-7	.2061e-8	.6437e-10	.2010e-11
6	.1245e-4	.1996e-6	.3100e-8	.4838e-10	.7578e-12	.5415e-12

TABLE 1. Implementation of all six schemes for a known solution: The maximum error in the L^2-norm (i.e. $\max_{0\le nk\le T}\|u^n-U^n\|$) of the approximate solution for various time steps is presented.

and the sixth order scheme is

$$
\begin{aligned}
&\left(\frac{147}{60}+k\mu_j\right)\hat{u}_j^{n+6}=6\left(1+\frac{1}{\nu}k\right)\hat{u}_j^{n+5}-15\left(\frac{1}{2}+\frac{1}{\nu}k\right)\hat{u}_j^{n+4}\\
&+20\left(\frac{1}{3}+\frac{1}{\nu}k\right)\hat{u}_j^{n+3}-15\left(\frac{1}{4}+\frac{1}{\nu}k\right)\hat{u}_j^{n+2}+6\left(\frac{1}{5}+\frac{1}{\nu}k\right)\hat{u}_j^{n+1}-\left(\frac{1}{6}+\frac{1}{\nu}k\right)\hat{u}_j^{n}\\
&-6k\widehat{(u^{n+5}u_x^{n+5})}_j+15k\widehat{(u^{n+4}u_x^{n+4})}_j-20k\widehat{(u^{n+3}u_x^{n+3})}_j\\
&+15k\widehat{(u^{n+2}u_x^{n+2})}_j-6k\widehat{(u^{n+1}u_x^{n+1})}_j+k\widehat{(u^{n}u_x^{n})}_j\,.
\end{aligned}
\tag{2.21}
$$

3. NUMERICAL EXPERIMENTS

In this section we present some numerical results of the implicit-explicit BDF schemes for the KS equation. We have performed the following experiments:

3.1. **Accuracy tests in a given time interval** $[0,T]$**.** We have carried out tests to establish the $p-$th order accuracy, for $p\in\{1,2,3,4,5,6\}$, of the corresponding $p-$step scheme for various time steps. We have thus obtained bounds for the time step which is required in order to achieve satisfactory accuracy. In these tests the numerical integration of the scheme was performed in the interval $[0,T]$, for a relatively small time T. All these experiments approximate the solution of an *inhomogeneous* problem of the form

$$
\begin{cases} u_t+u_{xx}+uu_x+\nu u_{xxxx}\,=\,f(x,t)\,,\\ u(x,0)\,=\,g(x)\,, \end{cases}
\tag{3.1}
$$

with a known solution. Both f and g are $2\pi-$periodic in space. The exact solution of (3.1) is taken to be $u(x,t)=\sin(x+t)$. In all experiments T was chosen to be 1 whereas $\nu=1/2$ and the number of modes 16. This number was determined from preliminary experiments, see Subsection 3.3. We used six different time steps, namely $k=\frac{1}{10},\frac{1}{20},\frac{1}{40},\frac{1}{80},\frac{1}{160},\frac{1}{320}$,

for all six schemes. We run the experiments using a double precision FORTRAN code (without external subroutine calls) on an IBM-6000 workstation.

Table 1 contains all the maximum errors in the L^2-norm, over the interval $[0,T]$, for all six schemes and all six time steps. All these data are presented in the `loglog` Figure 2. In both the table and the plot one can observe the $p-$th order of accuracy of the $p-$step method. The error in the case of the time step $\frac{1}{320}$ for the $6-$step method has not decreased as expected, since that would be beyond machine accuracy. It is noteworthy that the computation cost of BDF methods is independent of the number of steps.

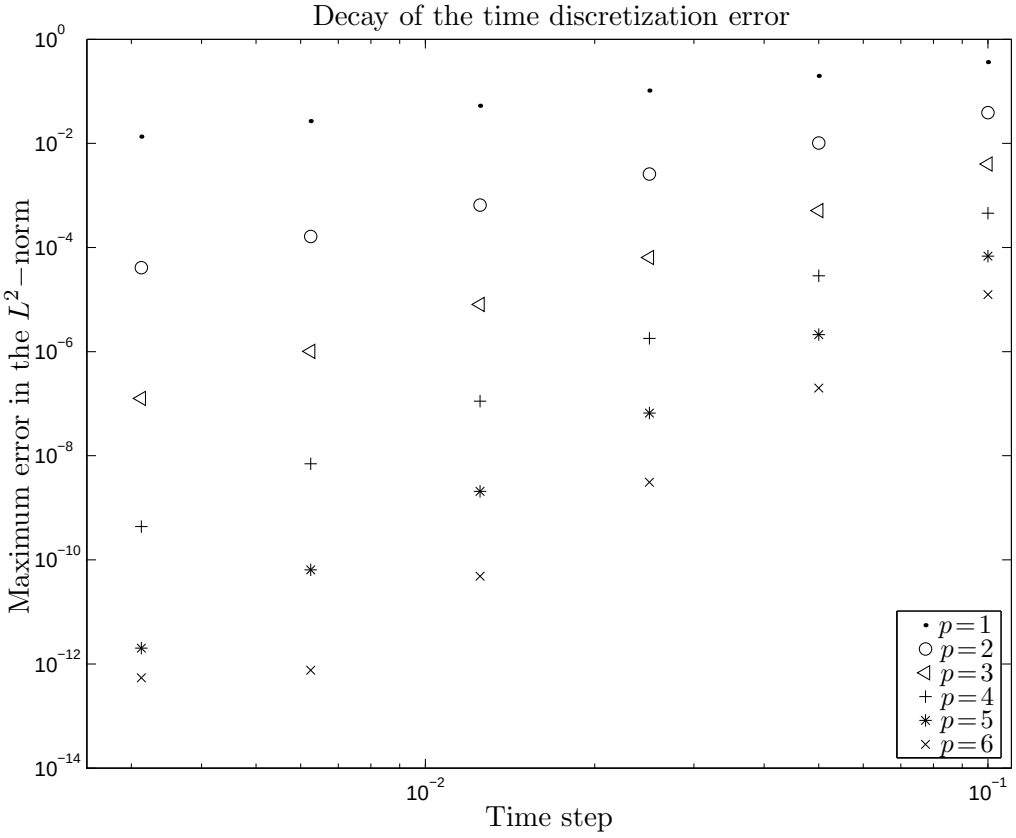

FIGURE 2. `loglog` plot of the maximum errors in the L^2-norm over the interval $[0,T]$ for various time steps

3.2. **Accuracy in the approximation of periodic attractors.** We have also carried out tests to establish the $p-$th order accuracy, of the $p-$step method, for $p \in \{1,2,3,4,5,6\}$, of the periodic universal attractors of the KS equation for various values of the parameter ν. Indeed, certain *computable* characteristics of universal attractors, such as the L^2-norm in the case of travelling waves and the period, in the case of periodic

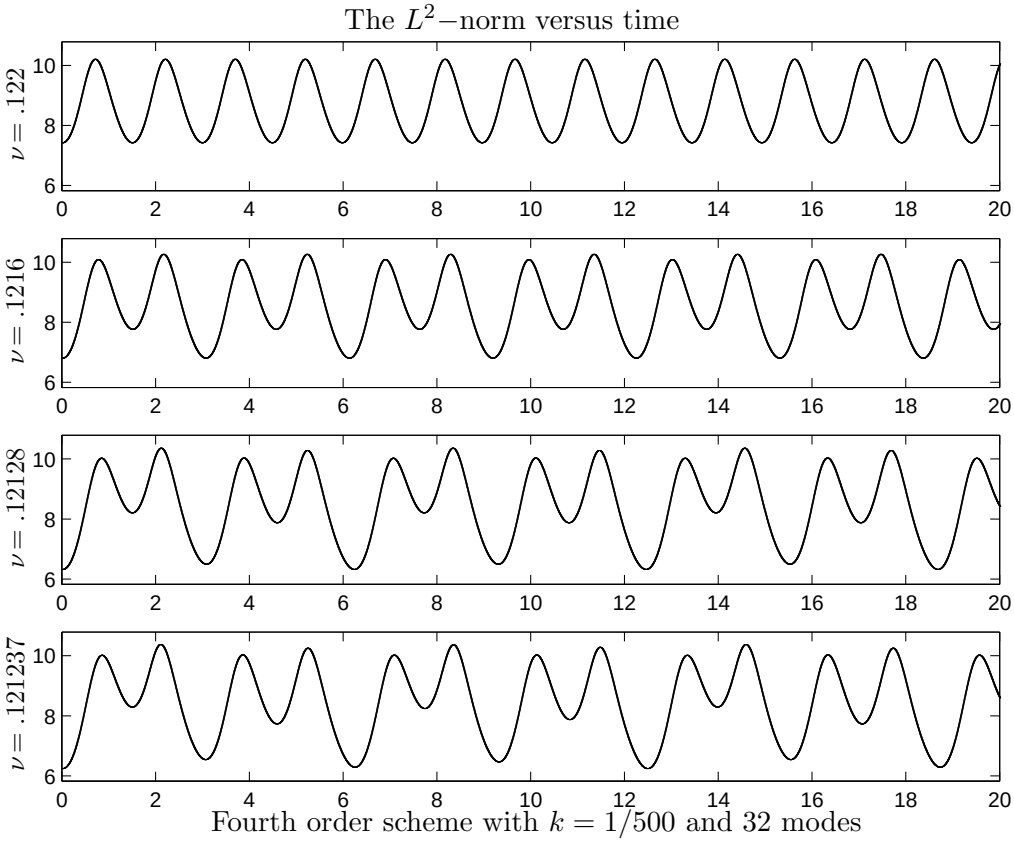

FIGURE 3. Three period doubling of the L^2-norm

attractors, appear to be approximated with the expected order of accuracy. Their qualitative characteristics are apparently obtainable with time steps larger than time steps in any other scheme used so far.

Table 2 provides the period of the periodic attractor (see Figure 4) at $\nu = .13$ for different time steps and for all the $p-$step methods. One can easily observe, at least for $p = 1, 2, 3$, that the order of accuracy in the calculation of the period is the same as the order of accuracy of the scheme. (For $p = 4, 5, 6$ the calculation of the period is *unfortunately* too accurate, and thus we can not observe any decay of the error.) It is noteworthy that the period of the attractor is measured from the period of the L^2-norm of the solution. The periodicity of the *Energy* or the L^2-norm, i.e. $E(t) = \|u(\cdot, t)\|$, can be seen in Figure 3. However, Figure 5 provides a much better evidence of periodicity since it contains six phase planes of the Energy, i.e. points $(E(t), E'(t))$, where $t \in [T_1, T_2]$. The derivative of $E(t)$ can be efficiently calculated from

$$\frac{d}{dt}\|u(\cdot,t)\|^2 = 2(u_t,u) = 2(uu_x + u_{xx} + \nu u_{xxxx}, u)$$
$$= -2(u_x,u_x) + 2\nu(u_{xx},u_{xx})$$

and thus

$$E'(t) \;=\; \frac{\nu\|u_{xx}\|^2 - \|u_x\|^2}{\|u\|}\,,$$

which is computed from the Fourier modes.

The phase planes correspond to six different values of the parameter ν. Closed curves correspond to periodic orbits. Finally, the period is measured by an extremely accurate method, consisting of approximating $E(t)$, near a t^* where its derivative vanishes, by a suitable polynomial, the coefficients of which are chosen via a weighted least square method. Newton's method subsequently provides the root, where the derivative of the polynomial vanishes.

Finally, we should report that, as with previous numerical experiments, certain chaotic phenomena have been identified. Specifically, period doubling cascade leading to chaos at $\nu \approx .121228053894\ldots$, following at least 14 period–doublings. In Figure 5, five period–doublings can be observed.

3.3. **Determining the number of Fourier modes.** The space discretization is achieved by truncating the high frequencies. This is quite plausible due to the analyticity of the solution and the exponential decay of the Fourier coefficients, see (1.5). We already have a rough idea of the rate of decay of these Fourier modes from the numerical estimates in [7]. Nevertheless, we have performed our own experiments in order to obtain similar estimates, see Figure 1. These specific preliminary experiments were performed in order to get a better idea of the number of modes with a significant numerical contribution to the solution. (Given that our codes are in double precision.) Clearly, this number is much larger than the number of the determining modes.

In order to achieve this, we used 64 modes and time steps significantly smaller than the ones used later and thus enabling even the high frequencies to develop individual behaviour. We tested the cases $\nu = .9,\ .5,\ .3,\ .2,\ .13,\ .1,\ .08,\ .05,\ .03$, and in each case we kept subdividing the time step until the `log−plot` of the spectrum stabilized. In the case of $\nu = .03$, we kept subdividing until the time step became $k = 10^{-8}$. Figure 1 provides these `log−plots` for selected cases.

4. Final remarks and possible extensions

The implementation of the BDF schemes for the numerical approximation of the solution of the KS equation has been very successful. These schemes allow us to use time steps larger than those previously used in order to achieve the desired accuracy and reproduce the already known asymptotic behaviour. However, when we use a larger time step for the approximation of the solution of infinite dimensional dynamical systems, which are

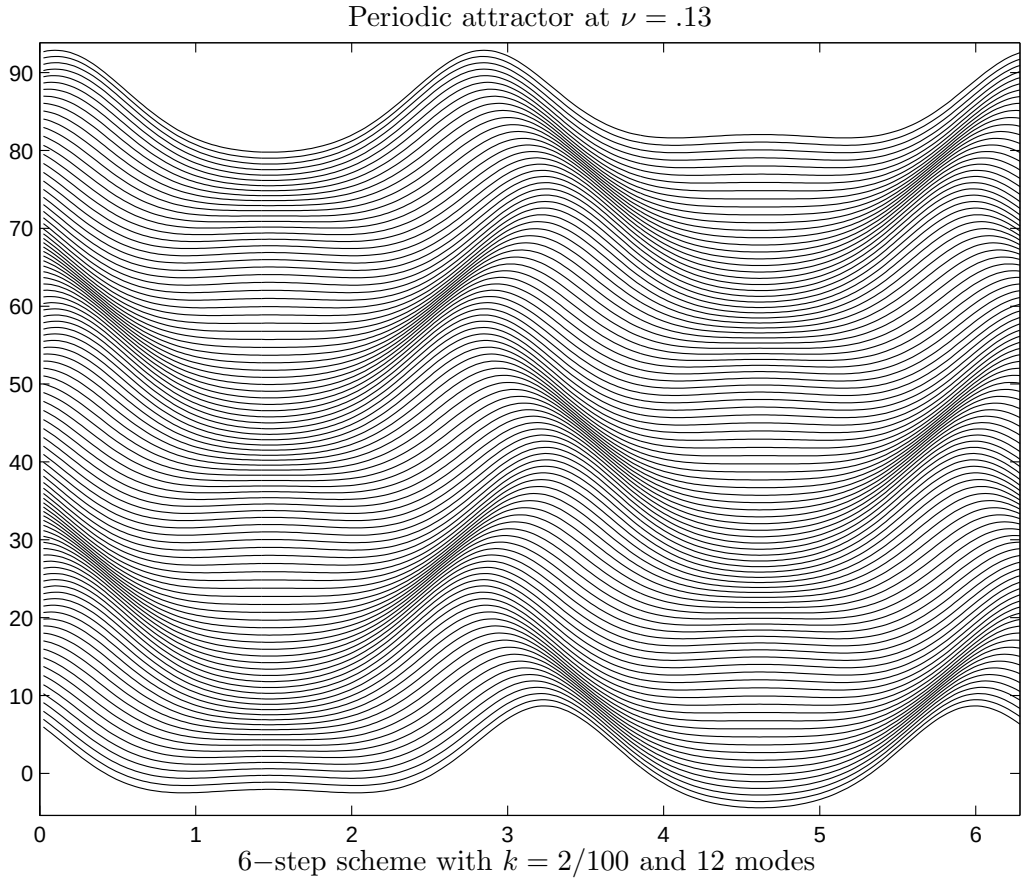

FIGURE 4. The evolution of the spatial shape of the approximate solution in a periodic attractor

characterized by stiffness, we lose the accurate approximation of high frequencies. Though stability in the integration of

$$\frac{d}{dt}\hat{u}_j \;=\; \lambda_j \hat{u}_j + \widehat{(uu_x)}_j\,,$$

for j large, is immediate due to the implicit integration of the linear part, in order to obtain good accuracy we need that

$$k|\lambda_j| \;=\; \Delta t|j^2 - \nu j^4| \ll 1\,, \tag{4.1}$$

which is extremely restrictive. However, higher order terms, due to their exponential decay, contribute gradually (as j grows) less to the solution and thus their relative accuracy becomes gradually less important. This fact compensates to the inherent stiffness of the system. Runs with extremely small time steps have been carried out with our schemes, in order to allow high frequencies to develop individual behaviour. However, no change in

	Number of steps of the BDF-scheme					
Time step	$p=1$	$p=2$	$p=3$	$p=4$	$p=5$	$p=6$
4/1000	1.057880776	.997326720	.996054681	.996066198	.996066355	.996066353
2/1000	1.026733486	.996380184	.996064879	.996066343	.996066353	.996066353
1/1000	1.011334827	.996144639	.996066168	.996066353	.996066353	.996066353
1/2000	1.003683672	.996085902	.996066330	.996066353	.996066353	.996066353
1/4000	.999870702	.996071238	.996066350	.996066353	.996066353	.996066353
1/8000	.997967440	.996067578	.996066353	.996066353	.996066353	.996066353
1/16000	.997016623	.996066647	.996066353	.996066353	.996066353	.996066353
1/32000	.996541420	.996066419	.996066353	.996066353	.996066353	.996066353
1/64000	.996303873	.996066372	.996066353	.996066353	.996066353	.996066353
1/128000	.996185096	.996066358	.996066353	.996066353	.996066353	.996066353

TABLE 2. The order of accuracy in the approximation of the attractors: Calculated period of the periodic attactor when $\nu = .13$.

the qualitative characteristics of the attractors was observed, and very little change in the quantitative ones. (See Table 2.) It turns out that the high frequencies are indeed slaved.

One could assert that, ideally the largest allowed time step, is the one having the property that, the relative error in any mode is inversely proportional to the contribution of this mode to the solution.

In our experiments, the time steps, though significantly larger than the ones used in previous experiments, are still small enough so that (4.1) holds for the determining modes and in fact for many more modes than the determining ones.

These methods could be efficiently applied for the numerical approximation of most infinite dimensional dynamical systems. In future work the method will be used in nonlinear evolution equations of parabolic type where the linear part can be integrated exactly.

REFERENCES

1. G. Akrivis, *High-order finite element methods for the Kuramoto-Sivashinsky equation*, RAIRO Modél. Math. Anal. Numér. **30** (1996) 157–183.
2. G. Akrivis and M. Crouzeix, *Linearly implicit methods for nonlinear parabolic equations*, Math. Comp. (to appear).
3. G. Akrivis, M. Crouzeix and Ch. Makridakis, *Implicit–explicit multistep finite element methods for nonlinear parabolic problems*, Math. Comp. **67** (1998) 457–477.
4. G. Akrivis, M. Crouzeix and Ch. Makridakis, *Implicit–explicit multistep methods for quasilinear parabolic equations*, Numer. Math. **82** (1999) 521–541.
5. U. M. Ascher, S. J. Ruuth and B. T. R. Wetton, *Implicit–explicit methods for time–dependent partial differential equations*, SIAM J. Numer. Anal. **32** (1995) 797–823.

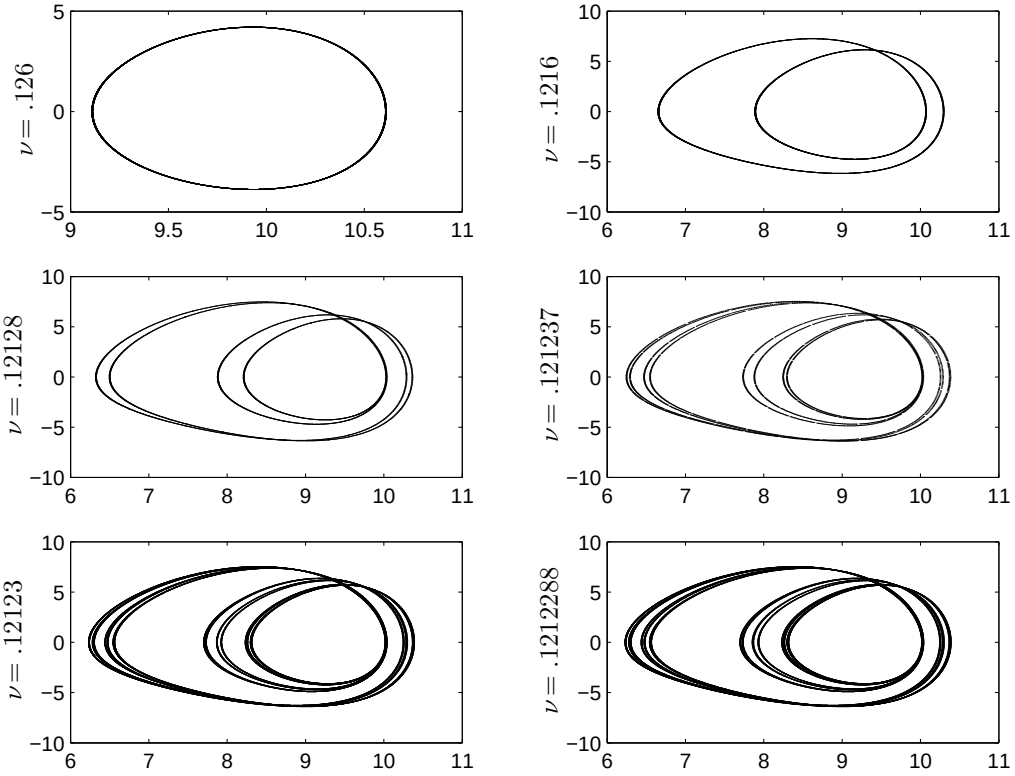

FIGURE 5. Phase plane of the L^2-norm: Five period doublings

6. P. Collet, J.-P. Eckmann, H. Epstein and J. Stubbe, *A global attracting set for the Kuramoto–Sivashinsky equation*, Comm. Math. Physics **152** (1993) 203–214.
7. P. Collet, J.-P. Eckmann, H. Epstein and J. Stubbe, *Analyticity for the Kuramoto–Sivashinsky equation*, Physica **D 67** (1993) 321–326.
8. P. Constantin, C. Foias, B. Nicolaenko and R. Temam, *Integral Manifolds and Inertial Manifolds for Dissipative Partial Differential Equations*, Springer–Verlag, New York, Appl. Math. Sciences, v. 70, 1988.
9. J. Goodman, *Stability of the Kuramoto–Sivashinsky equation and related systems. Analyticity for the Kuramoto–Sivashinsky equation*, Comm. Pure Appl. Math. **XLVII** (1994) 293–306.
10. E. Hairer, G. Wanner, *Solving Ordinary Differential Equations II: Stiff and Differential–Algebraic Problems*, Second Revised Edition, Springer–Verlag, Berlin Heidelberg, Springer Series in Computational Mathematics v. 14, 2002.
11. J. M. Hyman and B. Nicolaenko, *The Kuramoto–Sivashinsky equations, a bridge between PDEs and dynamical systems*, Physica **D 18** (1986) 113–126.
12. J. M. Hyman, B. Nicolaenko and S. Zaleski, *Order and complexity in the Kuramoto–Sivashinsky model of turbulent interfaces*, Physica **D 23** (1986) 265–292.
13. Ju. S. Il'yashenko, *Global analysis of the phase portrait for the Kuramoto–Sivashinsky equation*, J. Dynamics and Diff. Equations **4** (1992) 585–615.
14. M. S. Jolly, I. G. Kevrekides and E. S. Titi, *Approximate inertial manifolds for the Kuramoto–Sivashinsky equation: analysis and computations*, Physica **D 44** (1990) 38–60.

15. C. A. Kennedy and M. H. Carpenter, *Additive Runge–Kutta schemes for convection–diffusion–reaction equations*, Appl. Numer. Math. **44** (2003) 139–181.
16. I. G. Kevrekidis, B. Nicolaenko and C. Scovel, *Back in the saddle again: A computer assisted study of Kuramoto–Sivashinsky equation*, SIAM J. Appl. Math. **50** (1990) 760–790.
17. Y. Kuramoto, *Diffusion–induced chaos in reaction systems*, Suppl. Prog. Theor. Phys. **64** (1978) 346–367.
18. C. Lubich and A. Ostermann, *Linearly implicit time discretization of non-linear parabolic equations*, IMA J. Numer. Anal. **15** (1995) 555–583.
19. W. R. McKinney, *Optimal error estimates for high order Runge-Kutta methods applied to evolutionary equations*, Ph.D. thesis, University of Tennessee, Knoxville, 1989.
20. B. Nicolaenko and B. Scheurer, *Remarks on the Kuramoto–Sivashinsky equation*, Physica **D 12** (1984) 391–395.
21. B. Nicolaenko, B. Scheurer and R. Temam, *Some global dynamical properties of the Kuramoto–Sivashinsky equation: Nonlinear stability and attractors*, Physica **D 16** (1985) 155–183.
22. D. T. Papageorgiou, C. Maldarelli and D. S. Rumschitzki, *Nonlinear interfacial stability of cone-annular film flow*, Phys. Fluids **A2** (1990) 340–352.
23. D. T. Papageorgiou and Y. S. Smyrlis, *The route to chaos for the Kuramoto–Sivashinsky equation*, Theoret. Comput. Fluid Dynamics **3** (1991) 15–42.
24. G. I. Sivashinsky, *On flame propagation under conditions of stoichiometry*, SIAM J. Appl. Math. **39** (1980) 67–82.
25. Y. S. Smyrlis and D. T. Papageorgiou, *Computer assisted study of strange attractors of the Kuramoto-Sivashinsky equation*, Zeitschrift für Angewandte Mathematik und Mechanik **76**, number 2 (1996) 57–60.
26. Y. S. Smyrlis and D. T. Papageorgiou, *Predicting chaos for infinite dimensional dynamical systems: The Kuramoto–Sivashinsky equation, a case study*, Proc. Nat. Acad. Sc. **88** (1991) 11129–11132.
27. R. Temam, *Infinite–Dimensional Dynamical Systems in Mechanics and Physics*, Springer–Verlag, New York 1988.
28. V. Thomée, *Galerkin Finite Element Methods for Parabolic Problems*, Springer–Verlag, Berlin Heidelberg, Springer Series in Computational Mathematics v. 25, 1997.

Computer Science Department, University of Ioannina, 451 10 Ioannina, Greece
E-mail address: akrivis@cs.uoi.gr

Department of Mathematics and Statistics, University of Cyprus, 1678 Nicosia, Cyprus
E-mail address: smyrlis@ucy.ac.cy